NUMERICAL INVESTIGATION OF HEAT AND FLOW CHARACTERISTICS IN A LAMINAR FLOW PAST TWO TANDEM CYLINDERS

by

Neslihan AYDIN, Alper OZALP, and Irfan KARAGOZ *

Mechanical Engineering, Uludag University, Bursa, Turkey

Original scientific paper
https://doi.org/10.2298/TSCI201119175A

Heat and flow characteristics were investigated numerically for a laminar stream past two tandem circular cylinders placed in a channel. The blockage ratios ($\beta = D/H$) were chosen to be 0.6, 0.7, and 0.8, respectively, and the gap between the cylinders was varied proportionally to the cylinder diameter as g = 0.2D, 0.7D, 1.5D, and 4D at a low Reynolds number (Re = 40). The effects of the blockage ratio, as well as the gap between two cylinders on heat and flow features were examined in detail. Shear stresses, dimensionless static pressure, heat transfer coefficient, and separation points from the cylinders were determined from the velocity and temperature fields in the flow domain. The results showed that the separation angle decreases with both the blockage ratio and the gap size on the downstream cylinder, whereas heat transfer increases with both the blockage ratio and the gap size on the upstream cylinder.

Key words: *tandem cylinders, blocking effect, separation angle, drag coefficient, heat transfer*

Introduction

The flow of matter passing through bluff bodies in a channel is important in terms of the variability of the thermal and flow parameters. The flow characteristics around bluff bodies are encountered in many application areas [1-4]. Drag and drag reduction characteristics of these bodies were widely investigated by researchers in laminar flows [5-7]. Since the transfer processes are greatly affected by the flow structure around the bodies, many studies have focused on vortex shedding phenomena [8-10], instabilities and unsteady character of the flow [11-16] and vortex structure behind the bodies [17-20]. Some of these are also related to laminar flow [21, 22].

The flow around cylinders was numerically examined by Singha and Sinhamahapatra [23] for the values of Re = 40-150 and the gap g = 0.2-4D. It has been found that the flow rate and the blocking ratio significantly affect the separation point and the separation point goes backwards with the decrease in channel height. It has also been found that the change in channel height substantially affects the length of the recirculation zone. Kanaris *et al.* [24] examined the flow regimes by changing Reynolds number between 10 and 390 for the flow blocking ratio constant at 1/5. They observed that the flow regime passes from 2-D to

* Corresponding author, e-mail: karagoz@uludag.edu.tr

3-D flow regime between Re = 180-210 values. In addition, pressure coefficients and Strouhal numbers were calculated in this study.

The flow around cylinders of different diameters and the effects of cylinder sizes have also been investigated in the literature. Igarashi [25] attempted to determine the flow features around two cylinders with varying diameters by positioning the larger cylinder in front (big-small arrangement – BSA) for $d/D = 0.68$ and the cylinder spacing, $L/D = 0.9$-4. Flow characteristics and separation points were investigated by Alam and Zhou [26] for a stream around two cylinders with small-big arrangement, that is, the larger cylinder ($D = 25$ mm) at the rear and the front cylinder with $d = 0.24D$-$1D$. Gao *et al.* [27] studied the stability and unstable conditions for the flow around cylinders with dissimilar diameters designed in small-big arrangement. The effects of initial perturbation and the angular velocity of the front cylinder were examined for the Reynolds number of 200. They also tried to determine the critical spacing between the cylinders. Gao *et al*. [27] also worked on the fluid behavior nearby a pair of cylinders of dissimilar diameters by particle image velocity method. The distance between the cylinders as $L/D = 1.2$ and $d/D = 2/3$ were taken for Re = 1200. Under these values, flow regime and vortex formations were observed. Jiang *et al.* [28] investigated the flow nearby cylinders in BSA between two parallel walls, by using Lattice-Boltzmann method. The ratio between the cylinder diameters varied from 0.5 to 0.875. The influences of Reynolds number, diameter ratio, the distance between cylinders, and blockage ratio on the flow field were examined in detail. Numerical results have also been obtained in small-big arrangement and unconfined case.

Some researchers have studied heat and mass transfer characteristics as well as flow characteristics around cylinders. The flow around the cylinders was solved numerically by Zhou *et al.* [29] for moderate Reynolds numbers. In case of small gap, there is a stagnant flow around both cylinders. Furthermore, periodic vortex formations were observed in the second cylinder. Numerical results were obtained in this study by changing the Reynolds values between Re = 80-320 and the gap from $g = 2D$ to $8D$. Lavasani *et al.* [30] experimentally examined the values of Nusselt numbers, drag coefficients, pressure coefficients for an isothermal cam-shaped tube under forced heat transfer for $\mathrm{Re} = 7.5 \cdot 10^3$-$17.5 \cdot 10^3$ and blockage ratio of $1.5 \leq H/Deq \leq 7$.

Heat transfer studies in the literature are not detailed and exhaustive in low Reynolds number flows. A lot of research has been done on flows with different Reynolds numbers around a single cylinder or a single body. However, there is a gap in the analysis of the flows around Re = 40 where the vortexes start. Also, flows between multiple cylinders and interactions between cylinders have not been sufficiently studied. Hence, the novelty of this study is that the flow around tandem cylinders for Re = 40 was investigated at large blockage ratios and gap ratios between the cylinders. In this study, the effects of the gap ratio and blockage ratio on the flow structure, momentum, and heat transfer for Re = 40 are examined in detail by varying blocking ratio $\beta = 0.8$, 0.75, 0.7, 0.6 at different cylinder gap ratios $g = 0.2D$, $0.7D$, $1.5D$, $4D$.

Numerical method

Additional instructions

Basically, the continuity, momentum (Navier-Stokes equations) and energy equations need to be solved together with appropriate boundary conditions for the study of any flow. The conservation equations for the current study under the assumptions of steady, incompressible, and 2-D laminar channel flow are:

– continuity

$$\frac{\partial u}{\partial x}+\frac{\partial v}{\partial y}=0 \tag{1}$$

– momentum

$$\rho\left(u\frac{\partial u}{\partial x}+v\frac{\partial u}{\partial x}\right)=-\frac{\partial P}{\partial x}+\mu\left(\frac{\partial^2 u}{\partial x^2}+\frac{\partial^2 u}{\partial x^2}\right) \tag{2}$$

$$\rho\left(u\frac{\partial v}{\partial x}+v\frac{\partial u}{\partial y}\right)=-\frac{\partial P}{\partial y}+\mu\left(\frac{\partial^2 v}{\partial x^2}+\frac{\partial^2 v}{\partial y^2}\right) \tag{3}$$

– energy

$$u\frac{\partial T}{\partial x}+v\frac{\partial T}{\partial y}=\alpha\left(\frac{\partial^2 T}{\partial x^2}+\frac{\partial^2 T}{\partial y^2}\right) \tag{4}$$

The pressure distribution on the body due to the fluid motion, the aerodynamic forces, and vortex shedding in the wake of the body are all the aerodynamic characteristics.

A cylinder with a circular cross-section whose geometry looks simple, exhibits a highly complicated flow behavior when exposed to a flow environment. The flow structure around such a bluff body varies as a function of Reynolds number:

$$\mathrm{Re}=\frac{Ud}{\nu}=\frac{\rho Ud}{\mu} \tag{5}$$

which is a measure of the ratio of inertial forces to viscous forces. The viscous forces are the most important forces in the low Reynolds number flows and predominantly determine the fluid motion. There are certain flow-induced effects on bluff bodies in the flow field. These are the drag and lift forces acting on the object in the free flow direction and the perpendicular direction. Since the Reynolds number is quite low, the present study is mainly concerned with drag force. The resistance resulting from the viscous effects and the frictional forces is effective for the aerodynamic bodies such as aircraft wings, while the drag force due to the pressure difference becomes important for the bluff bodies.

The drag coefficient, C_D, of a cylinder is determined from the drag force, F_D, on the cylinder:

$$C_\mathrm{D}=\frac{F_\mathrm{D}}{\frac{1}{2}2\rho U^2 A} \tag{6}$$

where A is the projected area and U – the upstream velocity.

The pressure coefficient C_P is determined from pressure distribution over the cylinders:

$$C_\mathrm{P}=\frac{P-P_o}{\frac{1}{2}2\rho U^2} \tag{7}$$

where ρ is the density, P and P_o are the static pressure on the cylinders and at the outlet, respectively.

The Nusselt number is determined by:

$$\mathrm{Nu} = \frac{hD}{k} \tag{8}$$

where D, h, and k are the diameters of the cylinders, convection coefficient, and conduction coefficient over the cylinders, respectively.

Numerical analysis

The detail of the geometry and boundary conditions are given in fig. 1. The circular cylinders are centered between the adiabatic side walls in a channel. The non-slip boundary condition ($u = v = 0$) was applied to the adiabatic channel walls and the walls of the cylinders. The surfaces of the cylinders and the inlet air are given at constant temperatures T_s and T_∞, respectively.

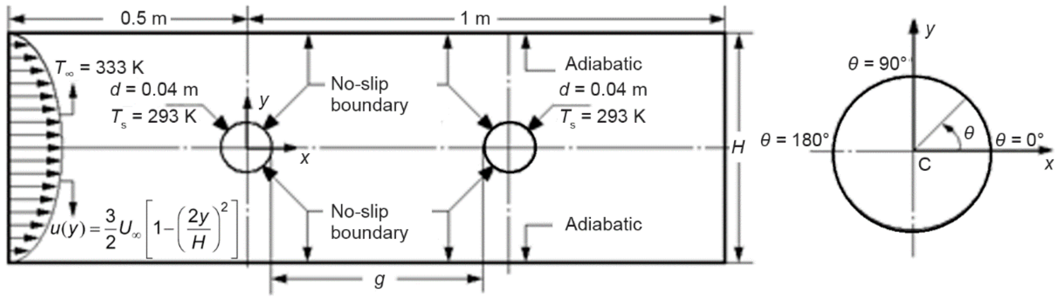

Figure 1. The flow area around the circular cylinders and the reference axis

The laminar air-flow was assumed as fully developed at the channel inlet and the parabolic velocity profile was used for the velocity inlet boundary condition. The U_C is the axial velocity of the air at the channel center. The temperatures on the cylinders were kept constant at T_s = 293 K, and the air temperature at the inlet was T_∞ = 333 K. Figure 1 also shows the positions of the back (downstream) and front (upstream) cylinders. The diameters of the cylinders were fixed to D = 0.04 m, the blocking ratios were taken as $\beta = D/H$ = 0.6, 0.7, 0.75, 0.8, and the gap between the cylinders was selected as g = 0.2D, 0.7D, 1.0D, 1.5D, 4D. The angular position around the 2-D circular cylinder is depicted by θ, fig. 1. Under these conditions, the conservation equations described above have been solved by means of the FLUENT software. The flow domain was discretized by hexahedra meshes and, a finer mesh was adopted around tandem cylinders comparing to the other region. Mesh independence study was carried out by creating meshes in different densities and number of nodes. The number of nodes 347250, 597104, and 786260 were tested. Since the changes in the results became negligible, the analyzes were continued with the number of 597104 nodes. The convergence criterion was $1 \cdot 10^{-7}$.

Results and discussion

Variation of separation angles with blockage ratio

Separation angle, θ_s, indicates the angle of the separation point on the cylinder, measured from the x-axis, fig. 1. The separation angles were obtained for two different blockage ratios and compared with [23, 31]. Separation angle for the blockage ratio of $\beta = 0.6$ was obtained as $\theta_s = 41.34°$ which is a very close value reported by Ozalp and Dincer [31]. When the blockage rate is reduced in the channel flow, in other words, when the channel height is increased, the separation angles increase on the upstream and the downstream cylinders. Table 1 shows the separation angles for $\beta = 1/24$ and a comparison with those given by Singha and Sinhamahapatra [23] over two cylinders with a distance g between them.

Both the present study and Singha and Sinhamahapatra [23] show that a reduction in the blocking rate from 0.6 to 1/24, led to an increase in separation angle of about 28%. Although Singha and Sinhamahapatra [23] observed a small effect of the second cylinder on the separation angle of the first cylinder, it remains unchanged for all g values studied in the present work. A very high angle of separation on the first cylinder (the upstream cylinder) directly affected the flow over the downstream cylinder and caused a lower angle of separation on this cylinder. As the gap between the cylinders, g, grows, the separation angle on the second cylinder slightly decreases to a certain point and remains constant after that. The results show that the influence of the first cylinder on the second one is dying out when the gap between the two cylinders is more than 3D. A comparison of the separation angles on the second cylinder shows that this study gives higher values for about 2% than the results stated by Singha and Sinhamahapatra [23] for the obstruction ratio of $\beta = 1/24$, tab. 1.

Table. 1 Separation angles on the front, f, and back, b, cylinders for $\beta = 1/24$

g	0.2D	0.7D	1.0D	1.5D	3D	4D
$\theta_{s\text{-f}}$	52.98	52.98	52.98	52.98	52.98	52.98
$\theta_{s\text{-b}}$	42.82	40.64	39.91	38.46	37.74	37.74
$\theta_{s\text{-f}}$ [23]	≅ 51.5	≅ 51	≅ 52	≅ 53	≅ 53.5	≅ 53.5
$\theta_{s\text{-b}}$ [23]	≅ 42	≅ 40.5	≅ 39.5	≅ 38	≅ 37	≅ 37

A parametric study was performed by altering the blockage ratio from 0.6 to 0.8, and the results are given in fig. 2. As can be understood from the figure, the separation angle on the upstream cylinder decreases as the blockage ratio rises, but it remains unchanged with the gap size, g, for all the distances studied.

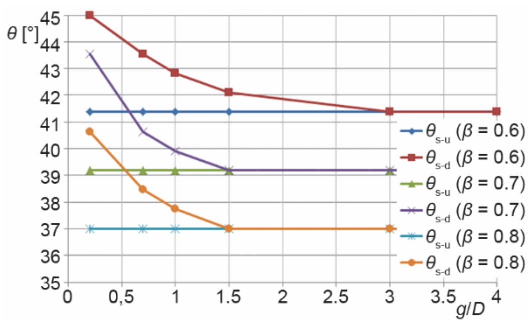

Figure 2. Separation angles on the front and back cylinders for blockage ratio = 0.6, 0.7, and 0.8
(*for color image see journal web site*)

On the downstream cylinder, the separation angle values are higher than those on the front cylinder due to the effect of the front cylinder. However, the separation angle on the back cylinder decreases to a certain point as the distance increases and then remains unchanged at the value of the separation angle on the front cylinder. That is, if the distance between the cylinders is higher than a specific amount, the separation angle on both cylinders equalizes. For example, the separation angle on the back cylinder decreases with the gap, starting from 45° at g = 0.2D to 41.37° at g = 3D where $\theta_{s\text{-f}} = \theta_{s\text{-b}} = 41.37°$ for $\beta = 0.6$. Similar behavior is also observed for the blockage ratios of 0.7 and 0.8 as can be seen in fig. 2. Therefore, it is possible to say that the effect of the front cylinder on the back cylinder dies out at the gap size larger than 1.5*D* and 3*D* for the blockage ratios of 0.8 and 0.7, respectively.

It is also confirmed from the temperature and velocity distributions around the cylinders that the front cylinder does not affect the back cylinder if the gap is higher than a particular value which is g = 1.5*D*, and 3*D* for $\beta = 0.6$ and 0.8, respectively. This means that the downstream cylinder is acting as a single cylinder if the gap, g, is larger than 1.5*D* for $\beta = 0.7$ and 0.8, larger than 3*D* for $\beta = 0.6$. As the blockage rate increases, in other words as the channel height decreases the separation angle decreases both on the front and back cylinders.

Pressure distributions on the cylinders

The variations of pressure coefficient on the front and back cylinders in the direction of flow are investigated, and results are given in fig. 3. Higher pressure coefficient values were obtained on the upstream cylinder. These values decrease by about half on the second cylinder. As the block rate increases from $\beta = 0.6$ to 0.8, the pressure coefficient values increase considerably on both cylinders. As can be seen from the figure, the pressure coefficient on the front cylinder is slightly influenced by the gap between the cylinders. This effect decreases with increasing blockage ratio. As the distance between the cylinders rises the pres-

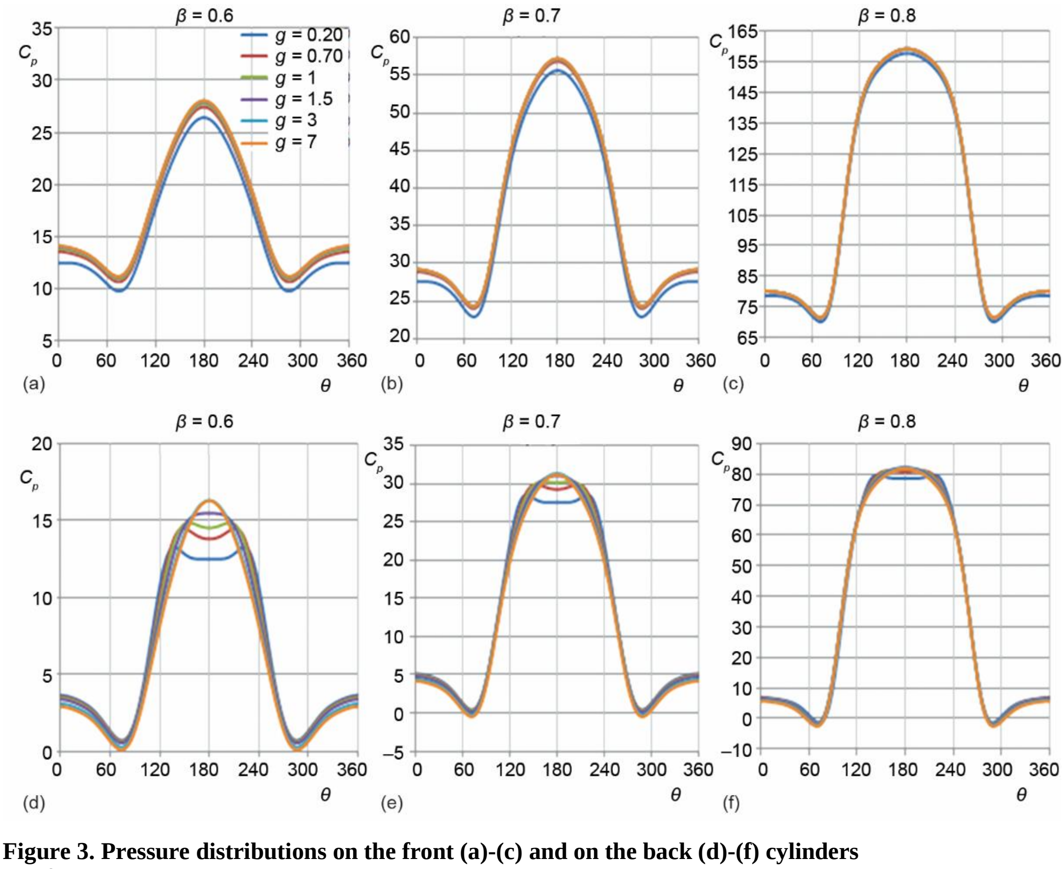

Figure 3. Pressure distributions on the front (a)-(c) and on the back (d)-(f) cylinders for $\beta = 0.6$, 0.8, and 0.7, respectively (*for color image see journal web site*)

sure coefficient increases on the front cylinders. This increase is negligible for higher blockage ratios. The maximum pressure coefficient appears in the stagnation point, $\theta = 180°$, on the upstream cylinder as $C_P = 160$ for $g = 4D$, and $\beta = 0.8$.

Similarly, the blockage ratio affects the pressure coefficient on the back cylinder. The gap between the cylinders affects mainly the pressure coefficient in front of the second cylinder. The change in the pressure coefficient exhibits a double peak curve around $\theta = 180°$. The effect of the gap decreases as the blockage ratio and the gap size increase. The downstream cylinder acts as a single cylinder when $g > 3$ that is the back cylinder is not influenced by the front cylinder, regardless of the block ratio. The pressure coefficient over the upstream cylinder changes between $C_P = 10$ up to 28.5 for $\beta = 0.6$. These extremum values increase to the values of 23-57 and 70-162 as the blockage ratio increases from $\beta = 0.7$ to $\beta = 0.8$, respectively. For the downstream cylinder, the distribution of pressure coefficient is between 0 and 17 for $\beta = 0.6$. As can be seen from fig. 3, C_P changes from positive to negative values for both $\beta = 0.7$ and 0.8 blockage ratios.

Heat transfer

Figure 4 shows the temperature contours in the flow field for all the cases studied. The temperature difference between the upstream and downstream sections increases with the blockage ratio, which demonstrates an increase in the total heat transfer rate. The mean temperature at the outlet is increasing with the blockage ratio while increasing with the gap. The effect of temperature variations produced by the front cylinder on the down stream cylinder dies out as the gap between the cylinders increases. Notably, for $g = 3D$ and $4D$ values, the temperature field in front of the downstream cylinder becomes nearly uniform. For the other gaps between cylinders ($g = 0.2D$, $0.7D$, $1D$, $1.5D$), the temperature change in the upstream cylinder affects the downstream cylinder.

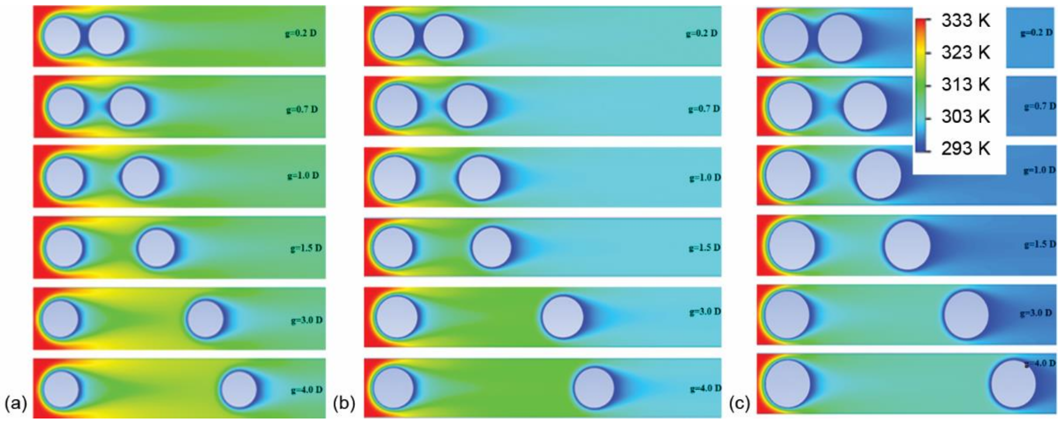

Figure 4. Temperature distribution around the cylinders for different gap size $g = 0.2D$, $0.7D$, $1.5D$, $3D$, and $4D$, respectively for blockage ratio; (a) $\beta = 0.6$, (b) $\beta = 0.7$, and (c) $\beta = 0.8$; Re = 40
(*for color image see journal web site*)

The temperature distributions around the upper and lower halves of the cylinders are symmetric and compatible with each other, due to the symmetry in geometry. The temperature between the two cylinders reaches 293, 303, 313, and 323 K for the gap values of $0.2D$, $0.7D$, $1D$, and $1.5D$, respectively. The temperature domain of influence of the cylinders also depends on the vortex structure. Therefore, the temperature variations around the cylinders show similar patterns with the velocity fields and the circulation regions.

As expected, the second cylinder leaves the domain of influence of the front cylinder as the gap increases. The increase in the blockage ratio draws this event to a shorter gap. Lower temperatures start to occur behind the downstream cylinder when the blockage ratio increases. As the channel height decreases, that is, as the blockage ratio increases, the temperature between the cylinders decreases. For example, the temperature between two cylinders does not exceed 313 K for $\beta = 0.8$, which is 323 K for $\beta = 0.6$.

Numerical values of the Nusselt number were deduced from the numerical results. Figure 5 demonstrates the variation of local Nusselt numbers over two cylinders. At first glance, the most striking feature is that the gap between the cylinders does not affect the local Nusselt number around the front cylinder except near the rear stagnation point for higher blockage ratios. The channel height at $\beta = 0.6$ is higher than the other blockage ratios, and convection heat transfer on the upstream cylinder has been a lot more for smaller gap sizes. The local Nusselt number reaches up to 8.5 for the conditions of $\beta = 0.6$ and $g = 0.2D$, $0.7D$, $1D$, $1.5D$. As the gap increases ($g = 3D$ and $4D$) the front cylinder is not influenced by the back cylinder and acts as if it were a single cylinder. The maximum Nusselt number slightly increases with the blockage rate increases around the upstream cylinder. It reaches a maximum value of 11.5 by showing two peaks at about $\theta = 100°$ and 260° for $\beta = 0.8$.

In the back cylinder, the effect of the front cylinder can be clearly seen at each blockage ratio. The local Nusselt number varies between 0.5 and 5 which are lower compared to the upstream cylinder. Heat transfer is falling considerably around the front stagnation point, $\theta = 180°$, when the gap decreases. However, a variation similar to the one in the front cylinder is observed in Nusselt number for $g = 3D$ and $4D$.

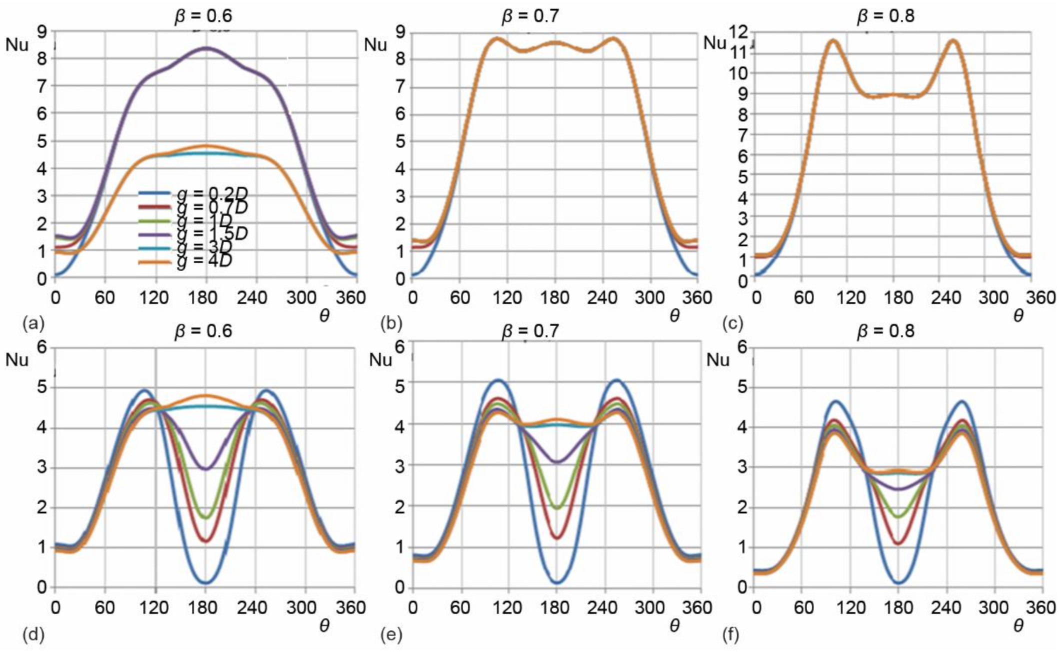

Figure 5. Nusselt numbers distributions on the front cylinder (a)-(c) and on the back cylinder (d)-(f) for β = 0.6, 0.7, and 0.8, respectively (*for color image see journal web site*)

Average Nusselt number over the cylinders were calculated and presented in fig. 6. In general, the average Nusselt number increases with the blockage ratio on the upstream cylinder and decreases on the back cylinder. It is not possible to say the same change for the effects of the gap. The average Nusselt number increases asymptotically with the gap size over both cylinders. The asymptotic values are 5.41, 6.06, and 6.88 on the upstream cylinder, and 3.22, 2.92, and 2.28 on the downstream cylinder at β = 0.6, 0.7, and 0.8, respectively. These asymptotic values on the upstream cylinder are reached at the gaps of 3*D*, 1.5*D*, and 1*D* for β = 0.6, 0.7, and 0.8, respectively. However, the corresponding gap values are 4*D*, 4*D*, and 3-D over the downstream cylinder.

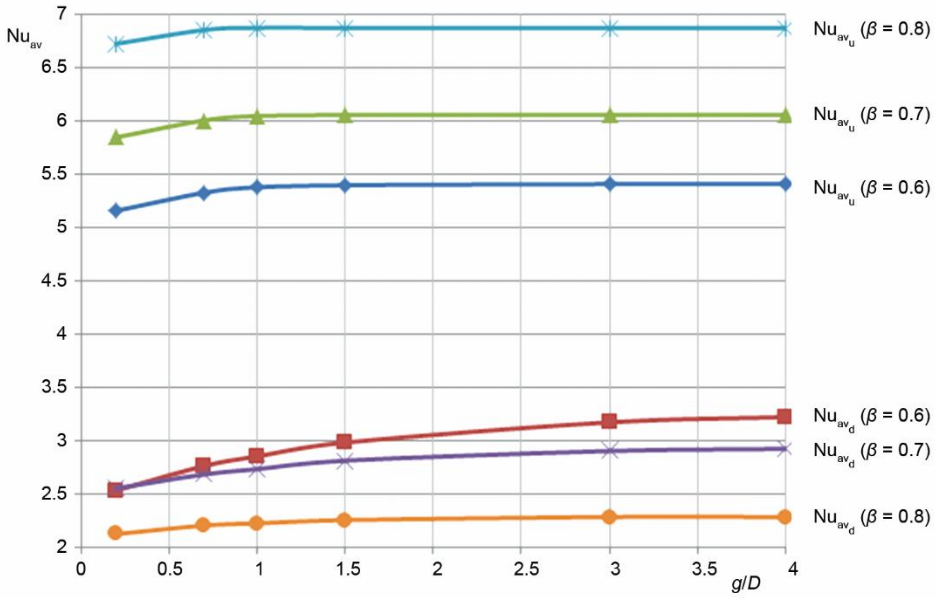

Figure 6. Variation of average Nusselt number *vs.* gap size; Re = 40
(*for color image see journal web site*)

Momentum transfer

Analysis of the flow field reveals that the velocity contours are very similar to temperature contours, fig. 7. It is observed that separations occur on the cylinder walls and the size of the circulation zones changes with the gap between the cylinders. The back cylinder remains in the circulation zone behind the front cylinder for smaller gaps such as g = 0.2*D*, 0.7*D*, 1*D*, 1.5*D* for β = 0.6. The flow behind the upstream cylinder is developing and becoming uniform as the gap increases, and the increase in the blockage ratio has an effect in favor of this uniformity. While the salvation distance of the downstream cylinder from the front vortex is 3*D* for β = 0.6, this value is 1.5*D* for the blockage rates of 0.8.

Pressure drag coefficients of two cylinders were calculated using eq. (6). The drag coefficients are increasing with both the gap and blockage ratio, being significant with the latter. The drag coefficient of the front cylinder increases slightly with the gap up to 2% which is negligible. The increase in the drag coefficient of the back cylinder is more pronounced, especially at small gaps. The effect of the upstream cylinder on the drag coefficient of the downstream cylinder is evident in small gaps. The drag coefficients of both cylinders increase considerably with the blockage ratio. The asymptotic values of the drag coefficient of the back cylinder are 0.89, 1.86, and 5.28 for the blockage ratios of 0.6, 0.7, and 0.8, respectively. Those values for the upstream cylinders are 0.92, 1.92, and 5.48.

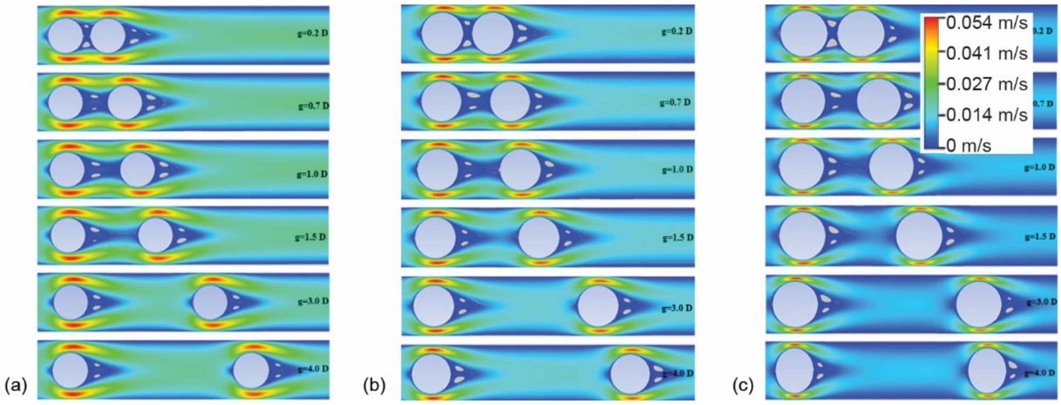

Figure 7. Velocity contours around the cylinders at Re = 40, for blockage ratio (a) β = 0.6, (b) β = 0.7, and (c) β = 0.8 (*for color image see journal web site*)

Conclusion

Flow and heat transfer parameters were studied numerically for a laminar flow around two cylinders in a channel by changing the blockage ratio and gap between the cylinders. The blockage ratios and the gaps between the cylinders were selected as the values that were rarely studied in the literature. The followings can be drawn from the results:

- A change in the gap between two cylinders does not affect the separation angle on the front cylinder. The same separation angle values are found at different gap sizes on the front cylinder. However, the separation from the wall on the upstream cylinder occurs earlier as the blockage rate decreases. The separation angle on the upstream cylinder changes from 41.37° to 37.01° when the blockage ratio increases from 0.6 to 0.8. The blockage ratio affects the separation on the downstream cylinder in the same way. Whereas, the separation angle on the downstream cylinder starts from a high value and decreases with the increase in the gap and reaches asymptotically to the separation angle on the upstream cylinder, regardless of the blocking rate.
- Drag coefficients for both cylinders increase considerably with the blockage ratio provided that the drag coefficient of the front cylinder is less than that of the back cylinder. However, the drag coefficient of the downstream cylinder increases slightly with the gap, whereas it remains unchanged on the upstream cylinder.
- Computational results also show that the blockage ratio and the gap between cylinders affect the temperature field considerably around the cylinders and heat transfer. The effect of the gap size on the local Nusselt number around the upstream cylinder is significant at small block ratios. The local heat transfer around the downstream cylinder slightly decreases with the blockage ratio. Whereas, the local Nusselt number values increase with the gap size, especially in front of the downstream cylinder.
- The average Nusselt number increases with the blockage ratio on the front cylinder and decreases on the back cylinder. However, the average Nusselt number increases

asymptotically with the gap size over both cylinders. The asymptotic values on the front cylinder are reached in shorter gap sizes. Increasing the blockage ratio helps to reach these values in shorter gap sizes for both cylinders.

Nomenclature

A –projected area, [m^2]
C_D – drag coefficient, [–]
C_P – pressure coefficient, [–]
D – diameter of the cylinders, [m]
F_D – drag force, [N]
g – gap size, [m]
h – convection coefficient, [Wm^{-2}K^{-1}]
H – channel height, [m]
k – thermal conductivity, [Wm^{-1}K^{-1}]
L – space between the cylinder axis, [m]
Nu – Nusselt number, [–]
Re – Reynolds number, [–]
P – pressure, [Pa]
T – temperature, [C]
u, v – velocity components, [ms^{-1}]
U – upstream velocity, [ms^{-1}]
U_C – axial velocity at the center, [ms^{-1}]

Greek symbols

α – correction energy factor, [–]
β – blockage ratio, [–]
θ – angular position of separation point, [°]
ρ – density, [kgm^{-3}]

Superscripts/subscripts

av – average
c – center
d – downstream
s – surface
u – upstream
o – outlet
s-f – separation of front
s-b – separation of back

References

[1] Gerrard, J. H., The Mechanics of the Formation Region of Vortices Behind Bluff Bodies, *J. Fluid Mech*., *25* (1966), 2, pp. 401-413
[2] Li, J., *et al.,* Numerical Study of Laminar Flow Past One and Two Circular Cylinders, *Comput. Fluids, 19* (1990), 2, pp. 155-170
[3] Wadcock, A. J., Bearman, P. W., The Interaction Between a Pair of Circular Cylinders Normal to a Stream, *J. Fluid Mech*., *61* (1977), 3, pp. 499-511
[4] Zdravkovich, M. M., Review of Flow Interference Between Two Circular Cylinders in Various Arrangement, *J. Fluids Eng*., *99* (1977), 4, pp. 618-633
[5] Chakraborty, J. P., *et al.,* Wall Effects in Flow Past a Circular Cylinder in a Plane Channel: A Numerical Study, *Chemical Engineering and Processing: Process Intensification*, *43* (2004), 12, pp. 1529-1537
[6] Sharman, B., *et al.,* Numerical Predictions of Low Reynolds Number Flow Over Two Tandem Circular Cylinders, *Int. Journal for Numerical Methods Fluids*, *47* (2005), 5, pp. 423-447
[7] Tsutsui, T., Igarashi, T., Drag Reduction of a Circular Cylinder in an Air-Stream, *Journal of Wind Engineering and Industrial Aerodynamics*, *90* (2002), 4-5, pp. 527-541
[8] Chang, K. S., Song, C. J., Interactive Vortex Shedding from a Pair of Circular Cylinders in a Transverse Arrangement, *Int. Journal for Numerical Methods in Fluids, 11* (1990), 3, pp. 317-329
[9] Farrant, T., *et al.,* A Cell Boundary Element Method Applied to Laminar Vortex Shedding from Circular Cylinders, *Computer and Fluids, 30* (2001), 2, pp. 211-236
[10] Griffith, M. D., *et al.,* Vortex Shedding and Three Dimensional Behaviour of Flow Past a Cylinder Confined in a Channel, *Journal of Fluids and Structures, 27* (2011), 5-6, pp. 855-860
[11] Chen, J. H., *et al.,* Bifurcation of Flow Past a Cylinder Between Parallel Planes, *J. Fluid Mech*., *284* (1995), Feb., pp. 23-41
[12] Jiang, R. J., Flow-Induced Vibrations Of Two Tandem Cylinders In A Channel, *Thermal Science*, *16* (2012), 5, pp. 1377-1381
[13] Jendrzejczyk, J. A., Chen, S. S., Stability of Tube Arrays In Circular Cylinders in Cross Flow, *Nuclear Engineering and Design*, *75* (1983), 3, pp. 351-373
[14] Johnson, A. A., *et al.,* Numerical Simulation of Flows Past Periodic Arrays of Cylinders, *Computational Mechanics*, *11* (1993), 5, pp. 371-383
[15] Kiya, M., *et al*., Flip-Flopping Flow Around Two Bluff Bodies in Tandem Arrangement, Bluff-Body Wakes, Dynamics and Instabilities, in: *IUTAM Symposium*, Springer-Verlag, Berlin, pp. 15-18, 1992

[16] Singh, S. P., Mittal, S., Flow Past a Cylinder: Shear Layer Instability and Drag Crisis, *Int. Journal for Numerical Methods in Fluids, 47* (2005), 1, pp. 75-98, 2005
[17] Rehimi, F., *et al.*, Experimental Investigation of a Confined Flow Downstream of a Circular Cylinder Centred Between Two Parallel Walls, *Journal of Fluids and Structures*, *24* (2008), 6, pp. 855-882
[18] Slaoutti, A., Stansby, P. K., Flow Around Two Circular Cylinders by the Random-Vortex Method, *Journal of Fluids and Structures*, *6* (1992), 6, pp. 641-670
[19] Williamson, C. H. K., Roshko, A., Vortex Formation in the Wake of an Oscillating Cylinder, *J. of Fluid and Structures*, *2* (1985), 4, pp. 355-381
[20] Zovatto, L., Pedrizetti, G., Flow about a Circular Cylinder Between Parallel Walls, *J. Fluid Mech*., *440* (2001), 1, pp. 1-25
[21] Meneghini, J. R., *et al.*, Numerical Simulation of Flow Interference Between Two Circular Cylinders in Tandem and Side-by-Side Arrangements, *Journal of Fluids and Structures, 15* (2001), 2, pp. 327-350
[22] Mittal, S., *et al.*, Unsteady Incompressible Flows Past Periodic Arrays of Cylinders in Tandem and Staggered Arrangements, *Int. J. for Numerical Methods in Fluids*, *25* (1997), 11, pp. 1315-1344
[23] Singha, S., Sinhamahapatra, K. P., High-Resolution Numerical Simulation of Low Reynolds Number Incompressile Flow about Two Cylinders in Tandem, *Journal of Fluids Engineering, 132* (2010), 1, pp. 1-10
[24] Kanaris, N., *et al.*, Three Dimensional Flow Around a Circular Cylinder in a Plane Channel, *Physics of Fluids*, *23* (2011), 6, ID 064106
[25] Igarashi, T., Characteristics of Flow Around Two Circular Cylinders of Different Diameters Arranged in Tandem, *Bull. JSME*, *25* (1982), 201, pp. 349-357
[26] Alam, M. M., Zhou, Y., Strouhal Numbers, Forces and Flow Structures Around Two Tandem Cylinders of Different Diameters, *J. Fluids Struct*., *24* (2008), 4, pp. 505-526
[27] Gao, Y. Y., *et al.*, Bi-Stable Flow Around Tandem Cylinders of Different Diameters at Low Reynolds Number, *Fluid Dynamics Research*, *43* (2011), 5, ID 055506
[28] Jiang, R., *et al.*, Numerical Prediction of Flows Past Two Tandem Cylinders of Different Diameters Under Unconfined and Confined Flows, *The Japan Society of Fluid Mechanics, Fluid Dynamics Research*, *46* (2014), 2, ID 025506
[29] Zhou, S., *et al.*, Numerical Study on Characteristics of Flow and Thermal Fields of Tandem Cylinders, *Heat Transfer Engineering*, *35* (2014), 11-12, pp. 1144-1151
[30] Lavasani, A. M., *et al.*, Effect of Blockage Ratio on Pressure Drag and Heat Transfer of a Cam-Shaped Tube, *Heat and Mass Transfer.*, *52* (2016), 9, pp. 1935-1942
[31] Ozalp, A. A., Dincer, I., Hydrodynamic-Thermal Boundary Layer Development and Mass Transfer Characteristics of a Circular Cylinder in Confined Flow, *International Journal of Thermal Sciences*, *49* (2010), 9, pp. 1799-1812

Paper submitted: November 19, 2020
Paper revised: April 2, 2021
Paper accepted: April 10, 2021